crystals

MDPI

Article

Control of 11-Aza:4-X-SalA Cocrystal Polymorphs Using Heteroseeds That Switch On/Off Halogen Bonding

Keyao Li [1], Monalisa Roy [1], Madiha Nisar [1], Lawrence W-Y. Wong [1], Herman H-Y. Sung [1], Richard K. Haynes [2] and Ian D. Williams [1,*]

[1] Department of Chemistry, Hong Kong University of Science and Technology, Clear Water Bay, Kowloon, Hong Kong, China
[2] Centre of Excellence for Pharmaceutical Sciences, North-West University, Potchefstroom 2531, South Africa
* Correspondence: chwill@ust.hk; Tel.: +852-2358-7384

Abstract: A family of: 1:1 cocrystals 11-Aza:4-X-SalA have been prepared from the potent anti-malarial compound 11-azaartemisinin with 4-halosalicylic acids. When X = 4-Cl, 4-Br and 4-I, two conformational polymorphs can be isolated in each case. Monoclinic type-I was found previously for parent 11-Aza:SalA (**1**) and 11-Aza:4-Br-SalA (**3a**) which have polar 2_1 stacks of molecular pairs with no short halogen bond contacts between stacks. Orthorhombic type-II is found for 4-Cl (**3b**) and 4-I (**4b**) from solution growth. This has a translational stack of molecular pairs involving a conformational change of the acid-lactam hetero-synthon and supramolecular association of stacks via halogen bonds. Notably, phase pure polymorph type-I can be formed for 4-Cl (**3a**) and 4-I (**4a**) by hetero-seeding with 11-Aza:SalA, whist conversely phase pure type-II for 4-Br (**2b**) can be formed using homo-seeding from liquid assisted grinding (LAG) product. This work demonstrates both the viability of engineering polymorphic cocrystal forms using hetero-seeds and the involvement of halogen bonds in helping to discriminate quite different polymorphic types.

Keywords: cocrystal; polymorph; hetero-seeding; liquid assisted grinding (LAG); artemisinin; anti-malarial drugs; conformational polymorph; Halogen bonds

Citation: Li, K.; Roy, M.; Nisar, M.; Wong, L.W.-Y.; Sung, H.H.-Y.; Haynes, R.K.; Williams, I.D. Control of 11-Aza:4-X-SalA Cocrystal Polymorphs Using Heteroseeds That Switch On/Off Halogen Bonding. *Crystals* **2022**, *12*, 1368. https://doi.org/10.3390/cryst12101368

Academic Editors: Venu Vangala and Srinivasulu Aitipamula

Received: 9 August 2022
Accepted: 20 September 2022
Published: 27 September 2022

1. Introduction

Recently we described the ability of the potent anti-malarial compound 11-azaartemisinin (11-Aza) [1,2] to form cocrystals with a wide variety of coformers [3]. Notably, for 20 carboxylic acids commonly used in drug formulation, around 50% of those screened formed a new cocrystal with 11-Aza [4–6]. These appeared to offer increased thermal stability and dissolution properties [4]. The driving force for cocrystallization appeared to be the formation of a robust $R_2^2(8)$ heterosynthon involving the acid C=O(OH) and amide NH-C=O of the 11-Aza lactam. In particular, the C=O---HO hydrogen bond was typically shorter (O---O <2.60A) than found in the related homosynthon dimers found in the parent acid crystals. This was particularly true for salicylic acid (SalA). Subsequently we have begun a systematic study using substituted salicylic acids (SalA-X) to see whether the tendency for cocrystal formation was more prevalent and whether small perturbations of the SalA-X molecular structure might affect the packing in the cocrystals of 11-Aza:SalA-X with a view to generating polymorphic structural arrangements [7].

For X = 4-Br, 5-Br and 3,5-Br_2 all three brominated salicylic acids formed 1:1 cocrystals from solution growth that were isostructural or homostructural with the parent unsubstituted cocrystal, with retention of polar 2_1-screw stacks of molecular pairs [6]. Herein we report that with X = 4-Cl or 4-I similar solution growth affords a quite altered packing arrangement involving molecular pairs with different heterosynthon geometry and simple translational molecular pair stacks.

Unlike the previously reported brominated phases, these show short X---X contacts that may be classified as halogen bonds. The details of the new cocrystal structure and our

successful efforts to use hetero-seeding [8–12] to influence the structure type and control the conformational polymorphism [13,14] of all three 4-halo substituted SalA-cocrystals with 11-azaartemisinin (Figure 1) will be discussed.

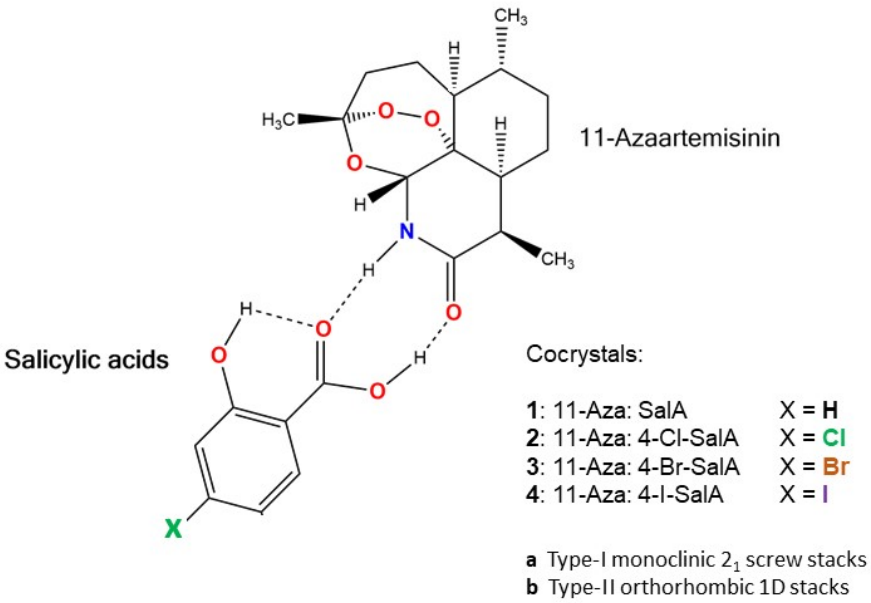

Figure 1. Molecular pairs of the 1:1 cocrystal phases of 11-azaartemisinin (11-Aza) and 4-X-salicylic acids (SalA-4-X), showing association through a lactam:acid heterosynthon.

2. Materials and Methods

Salicylic acids, artemisinin and solvents used were of reagent grade supplied by Meryer Chemicals, (Shanghai). 11-Aza was prepared from artemisinin by low temperature reaction with ammonia, following the modified method of Haynes et al. [15] of the original synthesis by Ziffer [1]. All new cocrystal phases can be obtained from liquid assisted grinding (LAG) [16], using a Tencan XQM-0.4A mini-planetary ball mill with zirconia vessels and media. A minimal amount of methanol (η factor = 0.2 mL/g) was used to accelerate the solid-state transformations which took between 30 min to 2 h [4]. Single crystals were grown by controlled evaporation at room temperature from methanolic solutions saturated with 11-Aza and containing slight excess of the salicylic acid. Specimen size for all the bromo and iodo containing compounds was kept small (<0.2 mm dimension) for single crystal X-ray diffraction to minimize absorption effects.

2.1. Preparation of Cocrystal Phases

2.1.1. 11.-Aza:SalA 1

This was prepared by LAG as a microcrystalline powder for seeding in hetero-templating experiments. 50 mg 11-azaartemisinin (~0.20 mmol, Fw 281.3) and 25 mg salicylic acid (25 mg, 0.2 mmol, Fw 138.1) were ground using zirconia media for 2 h using 0.075 mL MeOH (3 drops) to accelerate the phase transformation. The resulting white powder was inspected by P-XRD and consistent with previously published **1** 11-Aza:SalA, of type-I, with no peaks due to starting reagents remaining.

2.1.2. 11.-Aza:4-Cl-SalA **2a**

Type-I polymorph of **2** was prepared from controlled evaporation from 5 mL methanolic solution of 50 mg 11-Aza with equal mass (moderate excess) of 4-chlorosalicylic acid (CAS number 5106-98-90, Fw 172.6) that was seeded with around 5 mg of microcrystalline **1**. Care was taken that the seeds did not fully dissolve. The product was obtained after slowly evaporating the MeOH to less than 50% of the original volume. Work up of the resulting colorless tabular bar shaped crystals afforded 41 mg of phase pure **2a** (Fw 453.9,

45% yield). A small specimen of dimension 0.10 × 0.08 × 0.08 mm was selected for single X-ray diffraction.

2.1.3. 11.-Aza:4-Cl-SalA **2b**

Type-II polymorph of **2** can be prepared by LAG in a similar manner to the method for **1** above, or from controlled evaporation *without* hetero-seeding. For 50 mg 11-Aza scale and slight excess 4-chlorosalicylic acid this latter approach afforded colorless needles 45 mg of **2b** (Fw 453.9, 51% yield) and a specimen 0.15 × 0.10 × 0.10 mm was selected for single crystal X-ray diffraction.

2.1.4. 11.-Aza:4-Br-SalA **3a**

Crystals of **3a** (Type-I) were grown via controlled evaporation by the method described by us previously and with the crystal structure described [6].

2.1.5. 11.-Aza:4-Br-SalA **3b**

Microcrystalline **3b** was produced by LAG by the method described above for **1**, i.e., 50 mg 11-Aza and substituting 4-bromosalicylic acid (CAS number 1666-28-0, 44 mg, 0.2 mmol, Fw 217.0). Larger crystals of this could also be prepared using the microcrystalline **3b** powder as seeds for solution growth from MeOH by controlled evaporation, and this afforded a single crystal specimen 0.15 × 0.10 × 0.08 mm for single crystal structure analysis.

2.1.6. 11.-Aza_2:4-I-SalA **4a**

Microcrystalline **4a** was produced by LAG using the method described above for **1**, substituting 4-iodosalicylic acid (CAS number 16870-28-3, 55 mg, 0.2 mmol, Fw 264.0), in quantitative yield. The Powder-XRD revealed the structure of the new 1:1 cocrystal phase **4a** was of type-I, related to **1**, not **2b** or **3b**. Larger tabular single crystals of this phase could be produced by using seeding of this **4a** material or hetero-seeding with micro-crystalline **1**. In the latter case no contaminating presence of salicylic acid was found.

2.1.7. 11.-Aza_2:4-I-SalA **4b**

Solution growth following dissolution of 50 mg 11-Aza and same mass (slight excess) of 4-iodosalicylic acid via controlled evaporation of MeOH without seeding afforded a crop of single crystals of type-II polymorph **4b**. (53 mg, Fw 545.3, 49% yield) A needle 0.20 × 0.06 × 0.02 mm was selected for single crystal X-ray diffraction.

2.1.8. X-ray Crystallography

Powder X-ray diffraction data were obtained on cocrystal powders at room temperature using Cu-Kα radiation by a PanAlytical X'Pert PRO diffractometer with 1D X'celerator detector or on a PanAlytical Aeris benchtop powder X-ray diffractometer and measured in 2θ range 5 to 30° with step size of 0.02°. Single crystal X-ray structure determinations of the new phases **2a, 2b, 4a** and **4b** were carried out at 100 K on a Rigaku-Oxford Diffraction Supernova operating with a micro-focus Cu-Kα source and Atlas detector or Rigaku-Oxford Diffraction Gemini for structure **3b**. The structures were solved and refined using embedded SHELX programs [17,18] or internal options from within the Olex2 suite [19,20].

Structures refined successfully with solutions showing 1:1 cocrystal phases with two polymorph types found for **2**, **3** and **4**. Final discrepancy indices and bond length standard deviations were acceptably low and residual electron density was low except for absorption features associated with Br or I atoms. No disorder appeared present in these phases. Organic C-H hydrogens were placed geometrically with riding constraints and ADPs derived from the C atoms to which they were attached. All -CH and CH_2 groups had H-U_{iso} fixed at 1.2 times the C atom. Methyls were idealized as freely rotating CH_3 groups with H-U_{iso} fixed at 1.5 times that of the C atom. NH and OH were placed in geometric positions after confirming relevant electron peaks were located as expected. All cocrystal

structures are enantiopure solids based on incorporation of chiral 11-Aza which is derived from the sesquiterpene natural product artemisinin. The absolute structure parameters [21] of all five new phases clearly support the expected chirality due to the large anomalous scattering signal of Cl, Br, or I using Cu-Kα radiation.

Summary details of the crystal structure determinations for **2–4** are given in Table 1 for type-I polymorphs and Table 2 for type-II polymorphs. Unit cell data for the previously reported phases **1** and **3a** also measured at 100 K are included for comparison. The crystal structures of all the new phases have been deposited with the CCDC for inclusion in the Cambridge Structural Database and with deposition numbers in the tables.

Table 1. Crystal Data Summaries for **1**, **2a**, **3a** and **4a**, monoclinic polymorph type-I.

11-Aza:4-X-SalA	**X = H 1**	**X = Cl 2a**	**X = Br 3a**	**X = I 4a**
Reference	Ref. [4]	This work	Ref. [6]	This work
CCDC Number		2194192		2194193
Empirical formula	$C_{22}H_{29}NO_7$	$C_{22}H_{28}ClNO_7$	$C_{22}H_{28}BrNO_7$	$C_{22}H_{28}INO_7$
Formula weight	419.47	453.90	498.36	545.35
Temperature/K	100.01(10)	100.15	100.01(10)	100.15
Crystal system	monoclinic	monoclinic	monoclinic	monoclinic
Space group	$P2_1$	$P2_1$	$P2_1$	$P2_1$
a/Å	9.79451 (14)	11.0607(2)	11.0814 (2)	11.1497(2)
b/Å	9.30687 (13)	9.2616(2)	9.28293 (18)	9.3275(2)
c/Å	11.51291 (16)	11.0879(2)	11.1404 (2)	11.2726(2)
α/°	90	90	90	90
β/°	92.3070 (12)	97.941(2)	98.638 (2)	99.692(2)
γ/°	90	90	90	90
Volume/Å^3	1048.62 (3)	1124.95(4)	1132.99 (4)	1155.60(4)
Z	2	2	2	2
ρ_{calc}g/cm^3		1.340		1.567
μ/mm^{-1}		1.873		11.249
F(000)		480.0		552.0
Crystal size/mm^3		0.10 × 0.08 × 0.08		0.08 × 0.06 × 0.05
Radiation		CuKα (λ = 1.5418)		CuKα (λ = 1.5418)
2Θ range/°		8.052 to 153.55		7.956 to 153.236
Index ranges		$-11 \leq h \leq 13$, $-11 \leq k \leq 11$, $-13 \leq l \leq 13$		$-14 \leq h \leq 13$, $-10 \leq k \leq 11$, $-14 \leq l \leq 12$
Reflections collected		8337		7263
Independent reflecs.		4542		3859
Rint, Rsigma		0.0278, 0.0381		0.0258, 0.0345
Data/restr./params.		4542/1/285		3859/1/289
Goodness-of-fit F^2		1.029		1.033
Final R1, wR2, $I \geq \sigma(I)$		0.0300, 0.0738		0.0229, 0.0620
Final R [all data]		0.0326, 0.0762		0.0237, 0.0629
Res. peak/hole/e Å^{-3}		0.23/−0.17		0.34/−0.59
Flack parameter		−0.012(10)		−0.015(5)

Table 2. Crystal Data Summaries for **2b**, **3b** and **4b**, orthorhombic polymorph type-II.

11-Aza:4-X-SalA	**X = Cl 2b**	**X = Br 3b**	**X = I 4b**
Reference	This work	This work	This work
CCDC Number	2194194	2194677	2194195
Empirical formula	$C_{22}H_{28}ClNO_7$	$C_{22}H_{28}BrNO_7$	$C_{22}H_{28}INO_7$
Formula weight	453.90	498.36	545.35
Temperature/K	100.01(10)	100.01(10)	100.01(10)
Crystal system	orthorhombic	orthorhombic	orthorhombic
Space group	$P2_12_12_1$	$P2_12_12_1$	$P2_12_12_1$
a/Å	5.59110(10)	5.58020(10)	5.55980(10)
b/Å	15.0890(2)	15.2471(2)	15.7714(2)
c/Å	25.5977(3)	25.6542(3)	25.6306(3)
α/°	90	90	90
β/°	90	90	90
γ/°	90	90	90

Table 2. *Cont.*

11-Aza:4-X-SalA	X = Cl 2b	X = Br 3b	X = I 4b
Volume/Å^3	2159.53(5)	2182.71(6)	2247.44(6)
Z	4	4	4
ρ_{calc}g/cm^3	1.396	1.517	1.612
μ/mm^{-1}	1.952	2.950	11.568
F(000)	960.0	1032.0	1104.0
Crystal size/mm^3	0.15 × 0.15 × 0.1	0.15 × 0.10 × 0.08	0.2 × 0.06 × 0.02
Radiation	Cu Kα (λ = 1.54184)	CuKα (λ = 1.54184)	CuKα (λ = 1.54184)
2Θ range/°	6.8 to 145.046	6.71 to 141.78	6.58 to 144.876
Index ranges	$-6 \leq h \leq 6, -16 \leq k \leq 18, -29 \leq l \leq 31$	$-4 \leq h \leq 6, -17 \leq k \leq 18, -26 \leq l \leq 31$	$-6 \leq h \leq 5, -19 \leq k \leq 19, -28 \leq l \leq 31$
Reflections collected	12817	4709	12937
Independent reflecs.	4213	3350	4375
Rint, Rsigma	0.0298, 0.0287	0.0264, 0.0420	0.0306, 0.0283
Data/restr./params.	4213/0/285	3350/0/289	4375/0/285
Goodness-of-fit on F^2	1.019	1.041	1.037
Final R1, wR2 [I $\geq$ σ(I)]	0.0288, 0.0755	0.0270, 0.0652	0.0284, 0.0664
Final R [all data]	0.0303, 0.0770	0.0285, 0.0663	0.0288, 0.0666
Res. peak/hole/e Å^{-3}	0.23/−0.20	0.36/0.19	0.94/−1.04
Flack parameter	0.002(7)	0.017(15)	−0.011(3)

2.2. Differential Scanning Calorimetry

DSC measurements were made from ambient to 250 °C under a nitrogen atmosphere. on a Universal V4.5A TA Instrument (Waters). A heating rate of 10 °C per minute was employed using roughly 1 mg of sample for **2–4** type-I and type-II.

3. Results

3.1. Liquid Assisted Grinding (LAG) of Cocrystal Phases

Liquid assisted grinding (LAG) is a simple yet powerful preparative tool for checking the likelihood of co-crystal formation for pharmaceuticals and other organic compounds [16,22]. It is a mechano-chemical approach that can disrupt existing crystalline structures and provide a pathway to formation of new co-crystals. The addition of small quantity of suitable solvent can provide dissolution of starting solids to form saturated solution films on the surface of initial particles. The mechanical contact of these with solvated particles of the co-former can allow for solutions containing both components that are then able to nucleate and grow new co-crystal phases if these are thermodynamically preferred to the starting solids. Continued mechanical grinding keeps new exposed surface of the starting reagent particles to be uncovered until the transformation is complete. The approach was used to screen for cocrystal formation of artemisinin, which yielded just a few new co-crystals with polyphenolics like resorcinol, from around 80 co-formers tested [23].

We have found the conversion of the original lactone functionality of artemisinin to a lactam in 11-Aza provides more scope for co-crystal formation through favored intermolecular interactions [3–6]. Typically, screening for cocrystal formation with 11-Aza starts with a room-temperature liquid-assisted grinding (LAG) with a stoichiometric 1:1 mixture with the co-former. Typically new powder diffraction patterns were revealed after grinding for 1 h using zirconia media and 200 µL methanol per gram of solid. Little or no trace of starting reagents could be detected and isolated yields were effectively quantitative after grinding for 2–3 h.

In the case of salicylic acids SalA-X (X = 4-H, 4-Cl, 4-Br and 4-I) new product phases were formed in each case, giving cocrystal phases **1–4** respectively. (Figure 1) Complete conversion of starting coformers into products of 1:1 stoichiometry was found after around 1 h of grinding at 300 rpm, using a modest amount of MeOH solvent. The high success rate for co-crystal formation for salicylic acids [6] compared to organic acids in general, which

has just around 50% success [4], can be attributed to the strength of the heterosynthon for the highly acidic SalA-X, for which pKa_1 are typically less than 4.0.

The powder X-ray diffraction pattern for the parent co-crystal **1** (X = H) obtained from LAG was notably different from that of LAG products for X = Cl (**2b**) (Figure 2) and X = Br (**3b**) (Figure 3) which were apparently isostructural with each other. On the other hand, the powder diffractogram for LAG powder for X = I (**4a**) (Figure 4) showed a similar pattern to **1**. These results hinted that two distinct structural arrangements existed for these materials. In the case of 11-Aza:4-Br-SalA cocrystals seem to have at least two polymorphic forms I (**3a**) and II (**3b**), as the LAG powder gave a different pattern to that from the previously reported solution grown form.

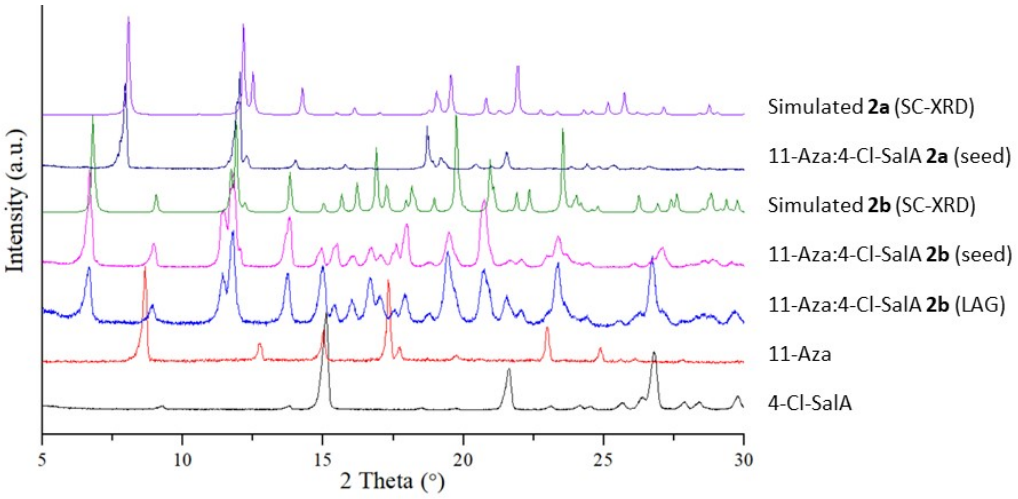

Figure 2. Powder X-ray diffractograms for **2a** (from solution growth after hetero-seeding with **1**) and **2b** from LAG along with the coformers 11-Aza and 4-Cl-SalA.

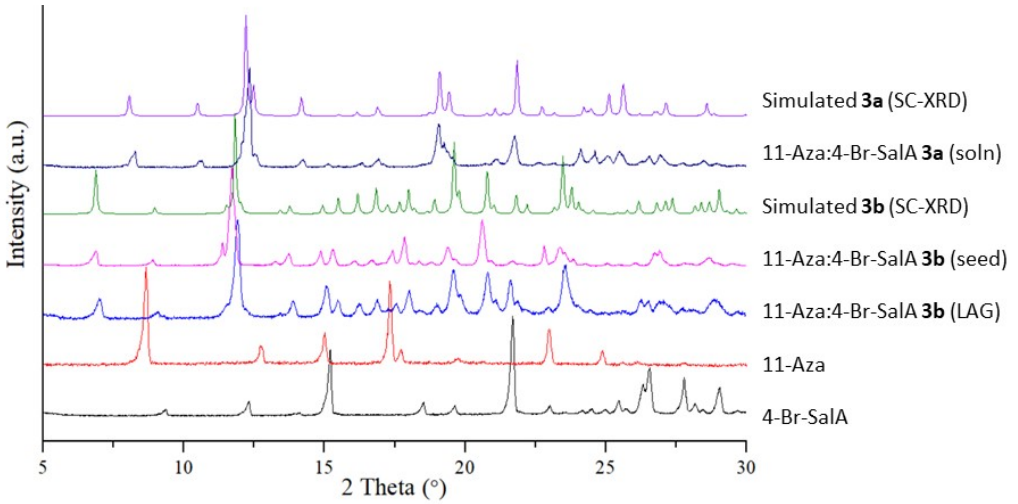

Figure 3. Powder X-ray diffractograms for **3a** (from solution growth) and **3b** from LAG along with the coformers 11-Aza and 4-Br-SalA.

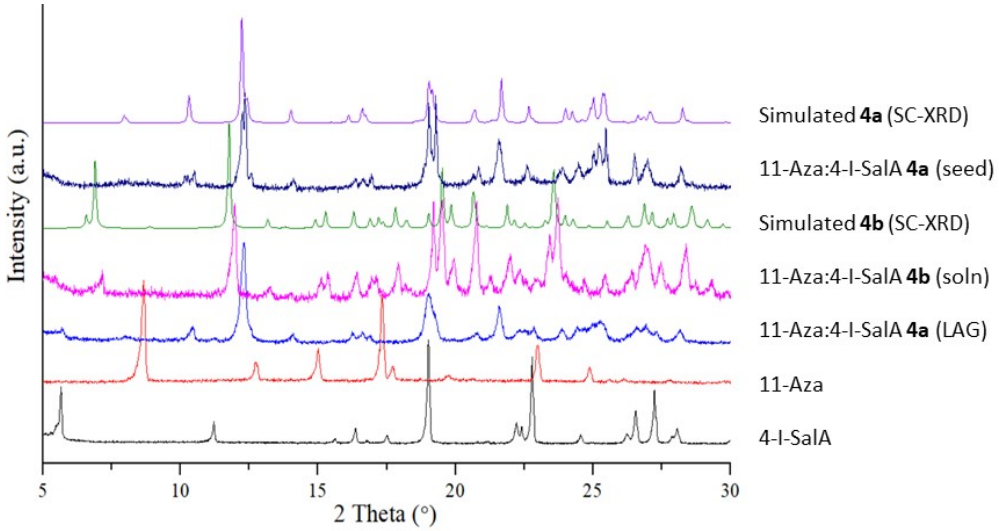

Figure 4. Powder X-ray diffractograms for **4a** (from solution growth after hetero-seeding with **1**) and **4b** from LAG along with the coformers 11-Aza and 4-I-SalA.

3.2. Initial Solution Growth of Single Crystals

The solution growth of the cocrystals 11-Aza:SalA (**1**) and 11-Aza:SalA-4-Br (**3a**) were previously reported using controlled evaporation of ethylacetate or methanolic solution [4,6]. A similar approach was now taken using 4-chloro and 4-iodo salicylic acids. Suitable specimens were grown from these systems and single crystal X-ray structure determination (Tables 1 and 2) revealed they belonged to new 1:1 cocrystal phases. In the case of X = 4-Cl the solution grown crystal was the same phase (**2b**) as was produced by LAG, however for X = 4-I the single crystal grown from solution (**4b**) was also isostructural with this, which was at odds with the LAG result.

Tables 1 and 2 summarize the structure determination details for cocrystals **1–4** 11-Aza:4-X-SalA where X = H (**1**), Cl (**2**), Br (**3**) and I (**4**). The cocrystal phases are given suffix **a** or **b** when referring to polymorphic form-I (monoclinic, parallel 2_1 screw molecular pair stacks) which are listed in Table 1 and form-II (orthorhombic, 1D translational molecular pair stacks) which are summarized in Table 2. The unit cell data for our previously published structures **1** and **3a** are included for completeness to aid comparison.

Although a strong acid:lactam $R_2^2(8)$ heterosynthon is found in all cocrystals, this has a different geometry for type-I and type-II so that the conformational arrangement of the molecular pair is altered and consequently the 3D packings are also quite distinct and unrelated to each other. A more detailed description of the structure types is given in the Discussion section below.

In summary both LAG and solution crystal growth for parent X = H gives monoclinic type-I phase, whereas for X = 4-Cl both LAG and solution crystal growth give a different form orthorhombic type-II. Rather unexpected discrepancies then exist for both the 4-Br and 4-I cases, that initially appear contradictory. In both instances there seem to be type-I and type-II polymorphs; however for X = 4-Br, type I is found by solution growth and type-II from LAG. Surprisingly the reverse situation is found for X = 4-I. These results hint that the two competing structure types are both thermodynamically similar and with competitive growth kinetics. We were interested to see whether all four systems could be induced to give both structural forms under suitable conditions.

3.3. Homo- and Heteroseed Templating of New Polymorphs

The structural discrepancy between the LAG prepared and solution grown forms of **3** and **4** led us to carry our further experiments to probe the crystallization outcome. Solution growth was carried out for **3** as before, but this time using seed crystals taken from the LAG product powder, which appeared to be of type-II. Previously we had found several

11-Aza acid co-crystal phases could be grown into large specimens by seeding solution growth with such LAG derived co-crystals. This worked in the case of several alkenoic acids, such as maleic and *trans*-cinnamic acid, that were hard to grow directly from mixed component solutions and prone to generating starting material crystals unless this seeding approach was taken [5].

In the case of 4-Br-SalA solution growth was redirected by addition of microcrystalline seeds of **3b** first obtained from LAG. After several days of controlled evaporation a large crop of 11-Aza co-crystals were harvested and the P-XRD of these were consistent with that of the LAG seeds and apparently phase pure. (Figure 3) A large good quality specimen was selected and S-XRD indeed confirmed both the unit cell and structure of the new polymorph II (**3b**) and which is isostructural with the 4-Cl and 4-I phases (**2b**) and (**4b**) as indicated in Table 2. In a similar way solution crystal growth for the 4-I system was reinvestigated. It was found that LAG produced microcrystalline powder of **4a** could serve as seeds for the growth of larger single crystal specimens and once more a phase pure sample of **4a** could be formed. (Figure 4) Its X-ray structure was determined and the details listed in Table 1.

The fact that the 4-Br and 4-I co-crystal could form two distinct polymorph types and that solution growth could be influenced by seeding encouraged the viewpoint that X = H and X = 4-Cl might also be able to adopt both structures if a hetero-seed was used. Hetero-nucleation is well established as a method of helping to control polymorph formation for API (Active Pharmaceutical Ingredient) systems [8–12]. Notably Jones et al. showed that phase diversity in cocrystal formation with respect to polymorphism and stoichiometry could be influenced by the methodology of growth, including grinding and seeding [8]. More recently, Price et al. have both advocated for, and practically demonstrated, the feasibility of using hetero analogues to provide a practical route to computationally predicted polymorphs that might otherwise be inaccessible [9,10].

In the case of the LAG prepared compounds **2–3** it is clear that the parent 11-Aza:SalA **1** has a different structural arrangement, albeit one that can also be similarly adopted by 11-Aza:4-Br-SalA **3a** by solution growth. We therefore attempted solution growth of the 11-Aza:4-Cl-SalA phase **2a** using hetero-seeds of LAG prepared **1** microcrystals. Harvesting these larger solution grown crystals after several days growth indeed afforded the new polymorphic form of type-I, 11-Aza:4-Cl-SalA **2a**. The powder XRD pattern of these were similar to the seeds of **1** and different from the LAG powder **2b** previously obtained. The hetero-seeded crystal structure was subsequently determined by S-XRD and confirmed the new **2a** form to be isostructural with our previously reported 4-Br analogue **3a**. Interestingly using microcrystals of **1** as a hetero-seed also worked for solution growth in the case of 11-Aza:4-I-SalA **4a**. Crystals grown this way are uncontaminated with parent SalA at the acid site of the crystal.

Apart from the powder X-ray diffraction patterns the crystal habits of the larger solution grown single crystals are reasonably distinct. Type-I crystals display a tabular bar-shaped morphology, whereas for type-II the aspect ratio is much larger and the crystals are best described as needles. Representative optical micrographs of the two types for X = Cl and X = I are shown in Figure 5. Thermal analysis of **2–4a** were compared to **2–4b**. The results in Figure 6 typically showed a small endothermic peak indicating melting, before a larger exothermic peak due to decomposition of 11-azaartemisinin between 150–160 °C. Slight higher thermal offsets support the idea that **2b**, **3b** and **4a** are the thermodynamically more stable phases.

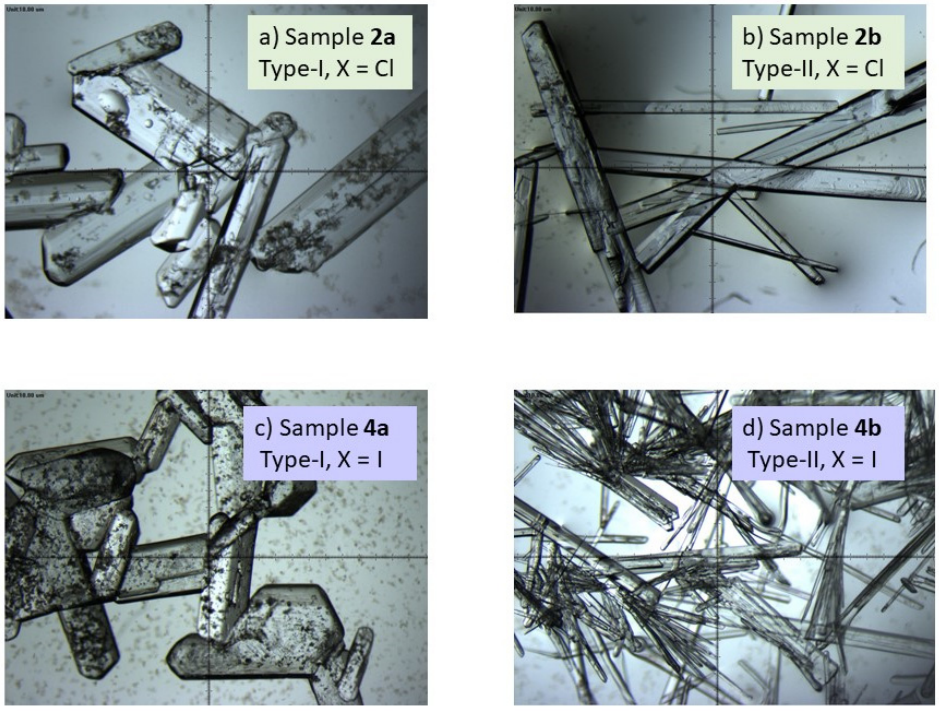

Figure 5. Optical micrographs of (**a**) **2a** 11-Aza: 4-Cl-SalA type-I, (**b**) **2b** 11-Aza: 4-Cl-SalA type-II, (**c**) **4a** 11-Aza: 4-I-SalA type-I, (**d**) **4b** 11-Aza: 4-I-SalA type-II. Large scale division = 10 microns.

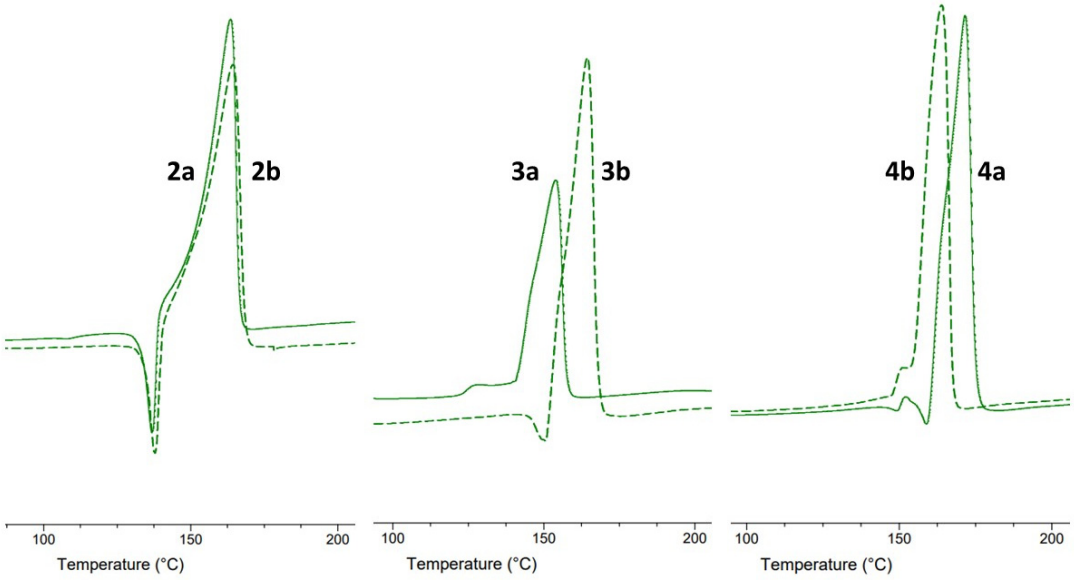

Figure 6. Differential scanning calorimetry (DSC) scans for phases **2–4** comparing (**a**) type-I (solid line) and (**b**) type-II (dashed line) forms.

Finally, attempts were made to hetero-seed growth of **1** using LAG derived **2b** or **3b**, but these were without success. The next section describes the structural differences between type-I and type-II in detail and suggests why the hetero-seeding of **1** to form a type-II polymorph is not successful.

4. Discussion

11-Azaartemisinin (11-Aza) is a potent anti-malarial compound [1,2], which has the potential advantage over commercial drugs in the artemisinin family in possessing a substantially greater half-life [24] and of not metabolising to dihydroartemisinin (DHA),

which has considerable neurotoxicity and is implicated in the mechanism of drug-resistance of *P. falciparum* parasites. Although 11-Aza has superior aqueous solubility to the parent artemisinin, the formation of various cocrystals is one important approach that can improve its dissolution kinetics and bioavailability. This approach is well-established for APIs and also offers other advantages in API fomulation [25,26].

Whilst artemisinin forms cocrystals only with some difficulty [23], our findings are that 11-Aza can form a quite wide variety of cocrystals and in particular with acids and these have been demonstrated to have superior dissolution kinetics and stability [3,4]. This is due to the formation of a robust heterosynthon between the lactam functionality of 11-Aza and the carboxylic acid. In general this allows around 50% of acids to form cocrystals with 11-Aza. In the case of salicylic acid (SalA) a particularly short O-H---O hydrogen bond of 2.55 Å was formed in the cocrystal 11-Aza:SalA. We therefore reasoned that this family of compounds would have a greater tendency for cocrystal formation and the wide availability of substituted salicylic acids (Sal-A-X) would allow us to probe the effects of simple atomic site substitutions on the packing of the cocrystals so formed.

In the case of several Br-substituted Sal-A-X, namely X = 4-Br, 5-Br and 3,5-Br_2, 1:1 cocrystals 11-Aza:SalA-X were formed that had structural similarity to the parent 11-Aza:SalA [6]. In extending these studies to other 4-halo salicylic acids X = 4-Cl and 4-I we have found that a quite different structure type. This exhibits a modified molecular geometry for the associated molecular pair. These are shown in Figure 7 for X = 4-Cl, phases **2a** and **2b**.

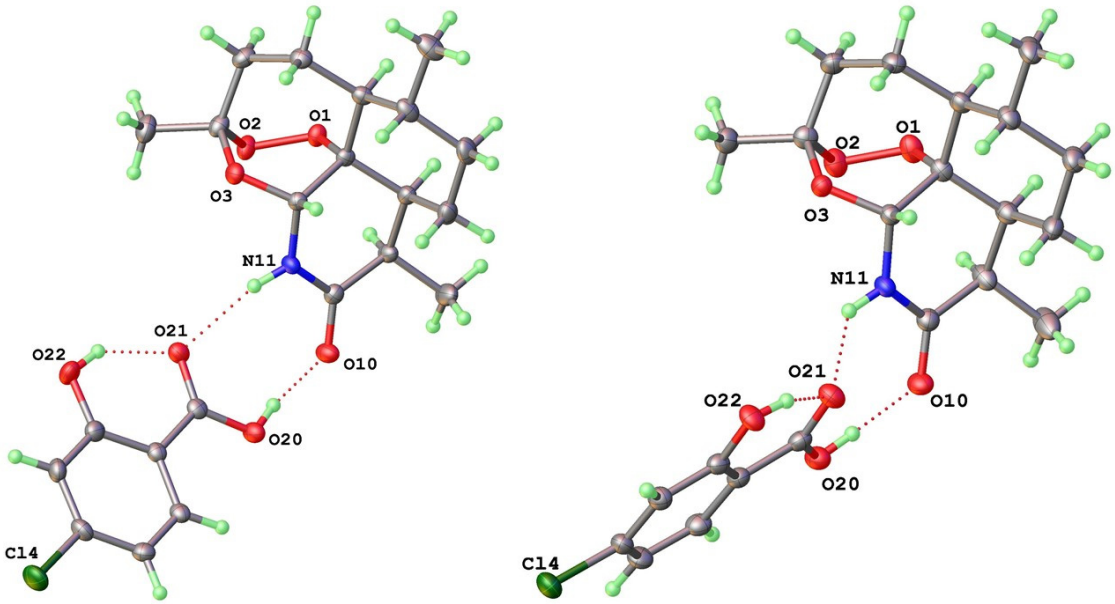

Figure 7. Variation in molecular pair conformations in crystal structure of 11-Aza:4-Cl-SalA, **2a** (Type-I) and **2b** (Type-II) (50% atomic displacement ellipsoids).

Through various studies of solution crystal growth, liquid assisted grinding (LAG) and experiments with homo- or hetero-seeding we have found that both structure types monoclinic type-I and orthorhombic type-II can be formed for all three halogens X = 4-Cl, 4-Br and 4-I. The parent 11-Aza:SalA (i.e., X = 4-H) cannot be induced into the type-II structure.

Although quite different from each other, clearly the two structure types are in general energetically competitive for the three halogens. The single crystal structures indicate that the structural difference can be traced back to the associative geometry of the molecular pair, although not the individual molecules themselves. 11-Aza itself is a polycyclic molecule with high degree of rigidity and salicylic acids are close to planar, since the intramolecular H-bond from the 2-phenol substituent keeps the carboxylic acid close the plane of the phenyl ring. The $R_2^2(8)$ heterosynthon (Etter notation) [27] then orients the keto oxygen (and thus

the 2-OH), but the geometry within the heterosynthon is different in type-I and -II. As indicated in Table 3 the N-H---O in type-II are shorter by around 0.08 Å, whilst the O-H---O distances within the synthon, which are more energetically important, are generically similar. Two characteristic intermolecular torsion angles C10-N11(H)---O21=C20 and C10=O10---(H)O20-C20 that traverse the synthon are quite different in the two structure types. The former has values of +50 and −59° and the latter +41 and −37° for type-I and II respectively. The relative difference amounts to a rotation of around 80° for the SalA-X relative to the 11-Aza molecule.

Table 3. Supramolecular geometric comparison for Type I (**a**) and II (**b**) polymorphs [1].

Distance(Å)/Angle(°)	2a 2b	3a 3b	4a 4b
N(11)H---O(21)	2.930	2.930	2.926
O(10)---HO(20)	2.852 2.555	2.841 2.551	2.839 2.561
	2.570	2.564	2.553
X---X [2]	4.632	4.643	4.668
	3.724	3.726	3.871
X---pi [3]	3.532	3.495	3.496
	NA	NA	NA
C(10)-N(11)---O(21)-C(20)	51.4	50.9	49.5
	−59.8	−59.4	−55.8
C(10)-O(10)---O(20)-C(20)	40.9	40.7	41.6
	−37.6	−37.6	−35.9
Specific Volume (Å^3)	562.5	566.5	577.8
	539.9	545.7	561.9
Difference ΔV (Å^3, %)	22.5, −4.0%	20.8, −3.7%	14.9, −2.8%

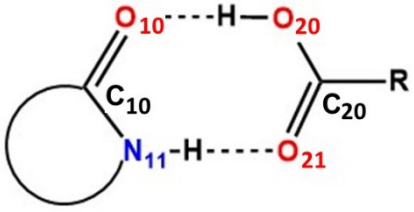

[1] Atom labels refer to the inset figure on the left and apply to both type-I and -II forms.
[2] X---X represents shortest halogen-halogen contact.
[3] X--pi represents halogen displacement from neighboring aromatic ring plane for type-I only.

The consequence of this geometric change is seen on the formation of the molecular pair stacks shown in Figure 8. In the two fold screw stacks of type-I the aromatic rings of the screw related SalA-X intercalate with the 11-Aza molecules, that are translated by 9.3 Å along the short b-axis of the monoclinic cell. By contrast, in type-II the rotation of the SalA-X allows the molecular pairs to assume a simple 1D translational repeat along the very short a-axis of around 5.6 Å.

By changing the molecular pair stacks the 3D structure is subsequently modified (Figure 9). Notably the polar stacks in type-I are arranged in parallel in a pseudo hcp arrangement of the columns, which we have discussed in an earlier paper [6]. As a consequence the entire crystal is polar. On the other hand the 1D translational stacks found in type-II crystals are polar themselves, but then form an embrace with a neighboring anti-parallel stack to form a rectangular column that then packs in a zig zag manner with neighboring columns to conform to the $P2_12_12_1$ space group.

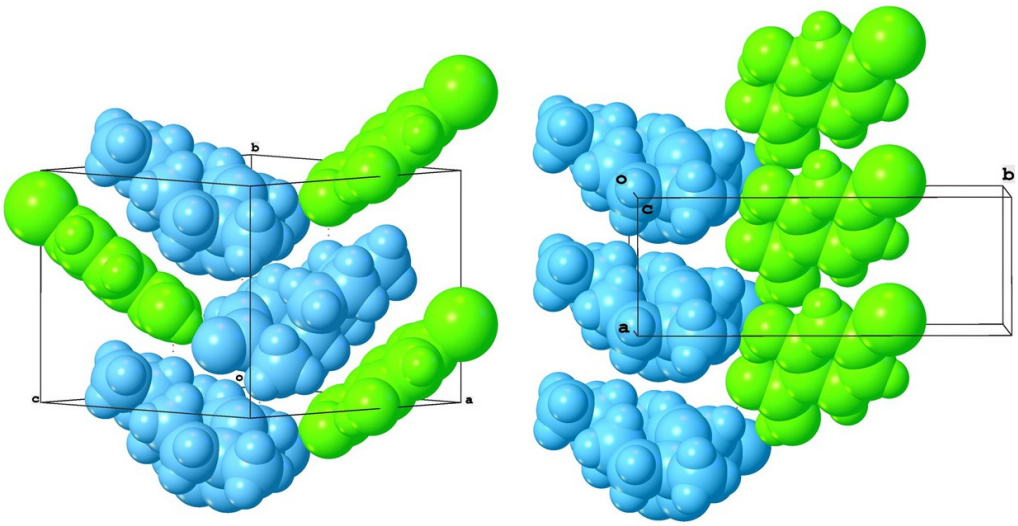

Figure 8. Two fold screw and translational molecular pair stacks in **2a** and **2b** respectively, showing unit cell and axes.

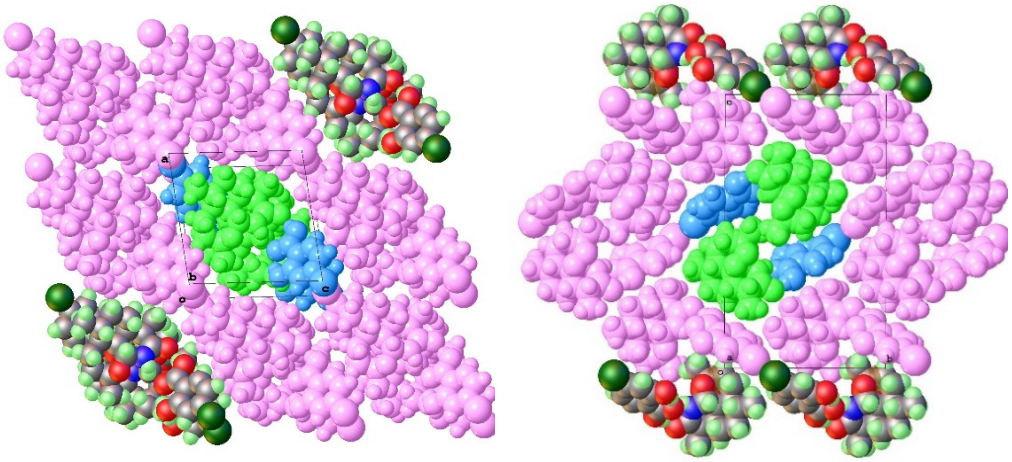

Figure 9. Packing of 11-Aza:4-Cl-SalA type-I (**left**) along [010] and type-II (**right**) along [100] showing supramolecular association of stacks.

One interesting consequence of the interactions between the stacks in the two polymorphs is the close interactions made by the halogens. As shown in Figure 10 the 4-halo-salicylic acids can self-associate as depicted for the 4-I case. In the type-I polymorph this interaction is primarily via a halo-phenyl close contact of a sigma hole-pi nature. The closest I---C non-bonded distance is around 3.54 Å, but orthogonal displacement of the I atom to the plane of the neighboring phenyl ring is just 3.496 Å. This has been depicted by the dashed line in the left hand side of Figure 10. In type-II cocrystals the twist of the salicylic acid molecules now places them in a zig-zag arrangement with respect to each other with short X---X contact. This halogen bond [28] is clearly *bona fide* in **4b** with I---I of 3.871 Å.

The relatively electron deficient sigma hole on the halogen which is opposite the terminal C-X bond can thus find favorable interaction with ether the pi-system or the electron rich band around a neighboring halogen. The strength of such inter-halogen bond typically increases with the polarizability of the halogen [28]. The X---pi and X---X distances in the type-I and II structures are listed, but must be compared with care. Thus the longer I---I of 3.871 Å found in **4b** is actually considerably shorter than 3.96 Å the sum of two van der Waals radii for iodine. For the related bromo case in **3b** the Br---Br distance is 3.726 Å, which is approximately equal to the van der Waals sum of 3.70 Å, whilst for chloro cocrystal **2b** the Cl---Cl of 3.724 is now slightly longer than the van der Waals sum of 3.50 Å.

Whatever positive attraction can occur between the pair of halogens is not the full story, since the competing interaction in phase type-I is halogen-pi in nature.

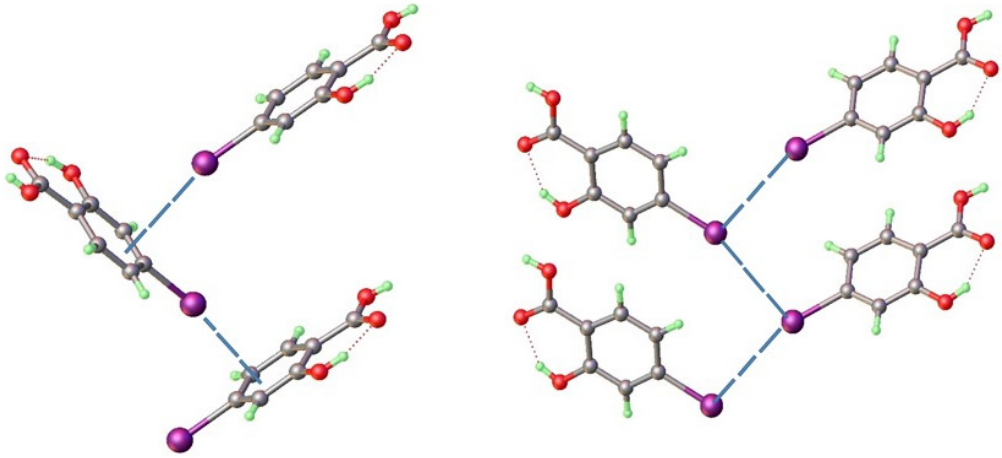

Figure 10. Closest iodo–iodo interactions are 4.668 Å in **4a** (**left**) and 3.871 Å in **4b** (**right**) respectively. Iodines in **4a** form short halogen σ-hole-π interactions of 3.496 Å, shown by dashed line.

In the type-I phases the shortest halogen—halogen distances are clearly non-bonding and approximately 0.9 Å longer than those found in type-II as indicated by the X---X entries in Table 3. The halogen-halogen and other interactions between the molecular pair surfaces with neighbors is usefully probed by Hirschfeld surface analysis fingerprint plots, shown in Figure 11, with the analysis conveniently carried out by Crystal Explorer [29]. The type-II cocrystals all show X---X component (highlighted in blue in Figure 11) whereas the type-I do not.

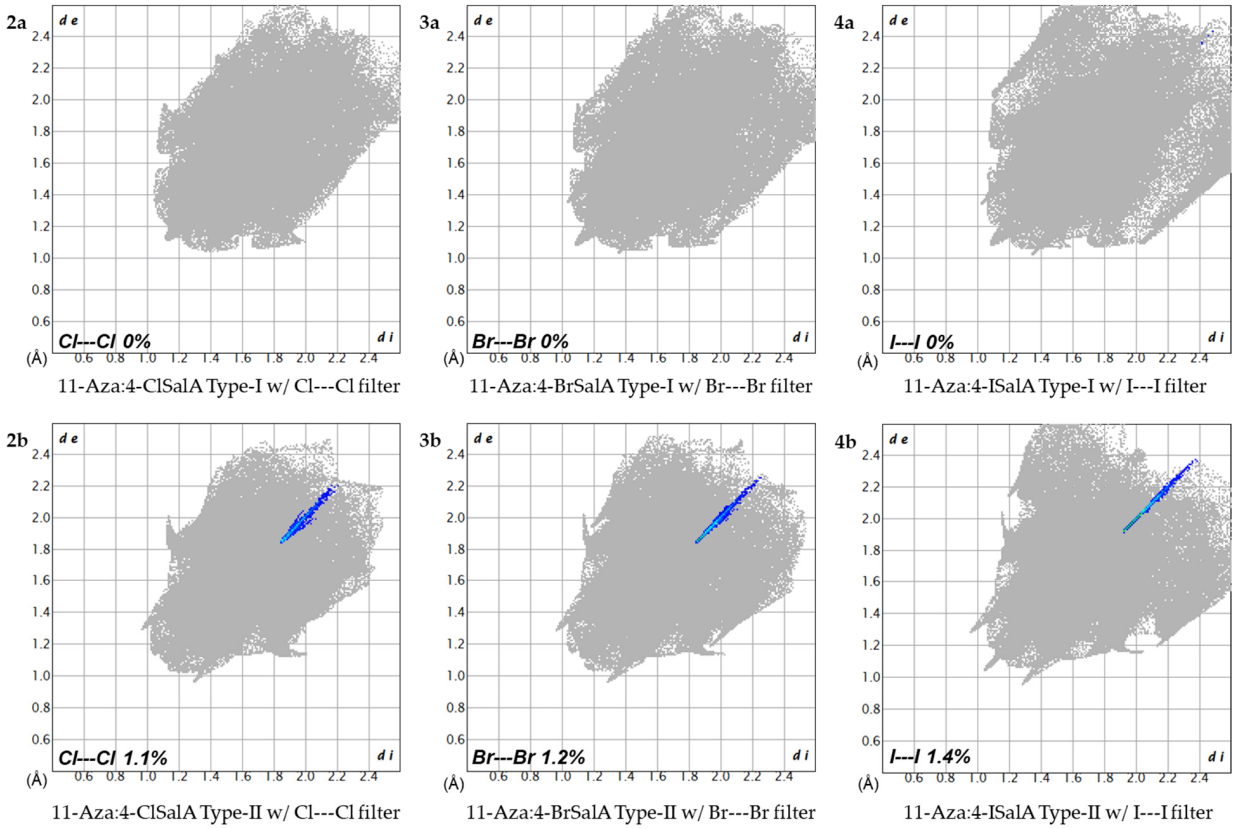

Figure 11. Hirshfeld surface analysis fingerprint plots [29] for Type-I **(upper)** and Type-II (**lower**) polymorphs of 11-Aza:4-X-SalA showing absence and presence of X---X interactions (**blue**).

Neither cocrystal shows any pi-pi stacking of aromatic rings, which would be indicated by C---C contacts of the Hirschfeld surfaces, but the X---C interactions are different and in type-I involves a greater percentage of the surface interaction. As shown in Figure 10 halogen-pi interactions are found to replace halogen-halogen ones in type-I structures. For type-I cocrystals the displacement of the halogen atom from the mean plane of the neighboring aromatic ring is listed as X---pi distance in Table 3. Interesting to note, this is longer for the smaller Cl atom (3.532 Å) and roughly identical in the Br (3.495 Å) and I cases (3.496 Å). Taking into account van der Waals radii this indicates this interaction is less favorable for Br than I and much less so for Cl.

The comparative energetics of the type-II phase with halogen bonds, compared to type-I analogues is clearly both of interest and significance when determining which phase is thermodynamically more stable under standard conditions. The results of LAG grinding might be expected to afford the thermodynamic product once equilibrium has been reached and completion of phase changes has occurred. It is thus notable that LAG afforded type-II for X =- Cl and Br but type-I for X = H and I. At first, we were surprised that the LAG product in the iodo case was type-I due to the fact that the relatively favorable halogen bond was lost. Careful studies using longer grinding times and varying solvent to ensure no further phase changes would occur were carried out and convinced us that type-I is probably the thermodynamic phase in this case, as is supported by the DSC results Figure 6. Our subsequent analysis of the X–pi interaction also being more favorable in the case of 4-I helps explain this initially surprising result.

The factors affecting the stability of cocrystal formation have been assessed recently by Taylor and Day [30] who point out that issues such as hydrogen bonds and halogen bonds may not be all-important and that packing volume is typically a more telling indicator. In cocrystal formation for 11-Aza we have found that the specific volume for molecular pairs in the cocrystals we have studied are generally equal to or less than the sum of the individual coformers from their parent crystals, when all are measured at the same temperature (100 K). Furthermore, the LAG results suggest that when cocrystals are formed these are thermodynamically preferred over the starting reagents, otherwise there is no driving force for phase transformation.

In the case of cocrystal polymorphs the comparison of energetics is more complex. However if the specific volumes (Table 3) are considered for phase types-I and II then the differences are quite revealing. Type-II is more efficiently packed for **2**, **3** and **4**, but the % difference decreases from X = Cl > Br > I. This is at least consistent with the notion that **2b** is strongly favored for X = Cl, **3b** slightly favored for X = Br and that **4a** (type-I) may be the thermodynamic phase for X = I. The DSC results shown in Figure 6 also support the idea that stability found for form-II for X = Cl and Br switches to form-I for X = I. The specific volume for **1** X = H is considerably smaller than the X = Cl type-I. Furthermore, because there would be no attractive X---X interaction in this case the C-H---pi interaction from the 4-H atom to neighboring ring found in type-I would appear to have a clear advantage over an edge-edge H---H interaction that would occur for type-II, even if the specific volume might be slightly smaller. It is likely that if type-I is thermodynamically favorable for **4** as we have conjectured, then this is strongly the case for **1**, to the extent that it cannot be induced via templating by hetero-seeds to give the type-II cocrystals.

The results described herein have some impact for the further development of functional cocrystals in a wider context. In the current system, we are continuing to explore the structural variations found by simple substitution of the salicylic acid ring. Since 3-, 4-, 5- and 6- substituted salicylic acids are either commercially available or may be synthesized, there is still considerable scope variation with just X = F, Cl, Br, I, Me, OMe, Et, that represent small changes in molecular size, shape and functionality with parent salicylic acid itself. There are also multiply substituted molecules, especially for 3,5-disubstitution and we have now characterized over twenty different 11-Aza:SalA-X cocrystals with over 90% success rate of formation. No other cocrystals in this family form type-II polymorph directly, though most others are also not of type-I, but typically have similar 2_1-screw stacks.

These all possess similar heterosynthon geometry to that found in type-I, indicating this is may be slightly more stable than the twisted heterosynthon found in type-II. Indeed this geometry is quite preserved to the cocrystals of 11-Aza with many other acids. The 2_1 screw stacks in type-I have parallel close packed arrays of stacks in a simple monoclinic $P2_1$ cell, in other cell types these are aligned in an anti-parallel, offset or helical manner to complete the 3D arrangement. This is the case for the 11-Aza:4-F-SalA, which has a tetragonal $P4_32_12$ structure.

This and other structures from these molecular SalA-X analogues represents other potential polymorphic forms. We are exploring the ability of these different structures to be adopted by hetero-seeding method we have described here. The computation of these polymorph stabilities for these 11-Aza:4-X-SalA cases will be an excellent test case for different parametric methods and it is hoped to then correlate these to experimental determination of dissolution and melting points. For 11-azaartemisinin the formation of suitable cocrystals such as with SalA may be of considerable help in its formulation and raising its bioavailability. Recent studies suggest the pharmacokinetics of 11-Aza is superior (t1/2 > 150 min) compared to current artemisinin based drugs, such as artemether (t1/2 = 17 min) [25] so its further development is warranted.

Considerable progress continues to made in the control, design and understanding of molecular solids. [31] This includes the ability to accurately compute polymorphic forms in an *ab initio* manner, [32] which may ideally be applied to the current cases discussed herein. Methods such as hetero-seeding with molecular analogues should grow in importance as they can provide a practical route to access such computed metastable solid forms for both APIs and their cocrystals [33]. It is notable therefore that the hetero-seeding with 11-Aza:SalA **1** can induce growth of type-I for X = Cl and I, while showing no residual contamination from the original hetero-seed compound. This supports earlier implications [8–10] for the general use of this method to access metastable polymorph phases for both APIs and API cocrystals, that can be energetically competitive, but for which no other direct preparative method is available. Further studies, particularly in the use of switching off/on halogen bonds or other structural features that can perturb the packing through single atom substitution are in progress.

5. Conclusions

Two polymorphic forms I (monoclinic) and II (orthorhombic) have been isolated in studies of cocrystals of the potent anti-malarial compound 11-azaartemisinin (11-Aza) with the 4-halo-salicylic acids 4-X-SalA for X = Cl, Br and I. Solution growth by controlled evaporation of either methanolic or EtOAc solutions of the coformers gives type I for X = Br (**3a**), homostructural with parent 11-Aza:SalA, (**1**) but affords type II for X = Cl and I (phases **2b** and **4b**). The type-I cocrystals for X = Cl and I (**2a** and **4a**) can however be grown by using seed crystals of the type-I 11-Aza:SalA (**1**) which were prepared by Liquid Assisted Grinding (LAG). Conversely for X = Br large type-II cocrystals (**3b**) can be prepared by self-seeding with microcrystalline **3b** obtained by LAG. Both polymorph types have lactam: acid heterosynthons that help drive cocrystal formation, but with quite different synthon geometry, so may be classified as conformational polymorphs. Type-II is likely to be thermodynamically preferred for **2–3** as it has smaller molar volumes due to better packing efficiency and the presence of significant X---X halogen bonds. Type-I appears preferred for **1** and **4** due to a less strained heterosynthon geometry and in the latter case what appears to be a favorable Iodo-pi interaction.

Author Contributions: Conceptualization, I.D.W., R.K.H.; methodology, M.N., L.W.-Y.W.; software, H.H.-Y.S.; validation, K.L., M.R. and L.W.-Y.W.; formal analysis, K.L., I.D.W.; investigation, K.L., M.N., M.R.; data curation, H.H.-Y.S.; writing—original draft preparation, K.L., I.D.W.; writing—review and editing, All.; supervision, I.D.W.; project administration, I.D.W.; funding acquisition, I.D.W., R.K.H. All authors have read and agreed to the published version of the manuscript.

Funding: This research was funded by Research Grants Council of Hong Kong (grant No. 16306515) (IDW); Hong Kong Branch of the Southern Marine Science and Engineering Guangdong Laboratory (Guangzhou) (grant No. SMSEGL-20SC01-D7) (IDW). This work was also supported by the South African Medical Research Council (MRC) Flagship Project MALTB-Redox with funds from the National Treasury under its Economic Competitiveness and Support Package (UID MRC-RFA-UFSP-01–2013) (RKH), and by a South African National Research Foundation (SA NRF) grant (UID 129135) (RKH).

Institutional Review Board Statement: Not applicable.

Informed Consent Statement: Not applicable.

Data Availability Statement: Crystal structure determinations have been deposited with the Cambridge Crystallographic Data Centre (CCDC) and available in the Cambridge Structural Database (deposition numbers given in Tables 1 and 2).

Acknowledgments: Ken Lau (City Univ., Hong Kong) is gratefully acknowledged for assistance with single crystal data collection and Fanny L-Y. Shek and Jane Y C. Wu for the DSC measurements.

Conflicts of Interest: The authors declare no conflict of interest. The funders had no role in the design of the study; in the collection, analyses, or interpretation of data; in the writing of the manuscript; or in the decision to publish the results.

References

1. Torok, D.S.; Ziffer, H. Synthesis and reactions of 11-azaartemisinin and derivatives. *Tetrahedron Lett.* **1995**, *36*, 829–832. [CrossRef]
2. Harmse, R.; Coertzen, D.; Wong, H.N.; Smit, F.J.; van der Watt, M.E.; Reader, J.; Nondaba, S.H.; Birkholtz, L.-M.; Haynes, R.K.; N'Da, D.D. Activities of 11-Azaartemisinin andN-Sulfonyl Derivatives against Asexual and Transmissible Malaria Parasites. *ChemMedChem* **2017**, *12*, 2086–2093. [CrossRef]
3. Nisar, M.; Haynes, R.K.; Sung, H.H.-Y.; Williams, I.D. Mechanochemical conversion of 11-azaartemisinin into pharmaceutical cocrystals with improved solubility. *Acta Crystallogr. Sect. A Found. Adv.* **2017**, *73*, a268. [CrossRef]
4. Nisar, M.; Sung, H.H.-Y.; Puschmann, H.; Lakerveld, R.; Haynes, R.K.; Williams, I.D. 11-Azaartemisinin cocrystals with preserved lactam: Acid heterosynthons. *CrystEngComm* **2018**, *20*, 1205–1219. [CrossRef]
5. Nisar, M.; Wong, L.W.-Y.; Sung, H.H.-Y.; Haynes, R.K.; Williams, I.D. Cocrystals of the antimalarial drug 11-aza-artemisinin with three alkenoic acids of 1:1 or 2:1 stoichiometry. *Acta Crystallogr. C Struct. Chem.* **2018**, *74*, 742–751. [CrossRef] [PubMed]
6. Roy, M.; Li, K.; Nisar, M.; Wong, L.W.-Y.; Sung, H.H.-Y.; Haynes, R.K.; Williams, I.D. Varying degrees of homostructurality in a series of cocrystals of antimalarial drug 11-azaartemisinin with salicylic acids. *Acta Crystallogr. Sect. C Struct. Chem.* **2021**, *77*, 262–270. [CrossRef] [PubMed]
7. Williams, I.; Li, K.; Sung, H.H.-Y.; Roy, M.; Nisar, M. Towards engineering the polymorphs of cocrystals. *Acta Crystallogr. Sect. A Found. Adv.* **2020**, *76*, a25. [CrossRef]
8. Trask, A.V.; van de Streek, J.; Motherwell, W.D.S.; Jones, W. Achieving Polymorphic and Stoichiometric Diversity in Cocrystal Formation: Importance of Solid-State Grinding, Powder X-ray Structure Determination, and Seeding. *Cryst. Growth Des.* **2005**, *5*, 2233–2241. [CrossRef]
9. Srirambhatla, V.K.; Guo, R.; Price, S.L.; Florence, A.J. Isomorphous template induced crystallisation: A robust method for the targeted crystallisation of computationally predicted metastable polymorphs. *Chem. Commun.* **2016**, *52*, 7384–7386. [CrossRef]
10. Case, D.H.; Srirambhatla, V.K.; Guo, R.; Watson, R.E.; Price, L.S.; Polyzois, H.; Cockcroft, J.K.; Florence, A.J.; Tocher, D.A.; Price, S.L. Successful Computationally Directed Templating of Metastable Pharmaceutical Polymorphs. *Cryst. Growth Des.* **2018**, *18*, 5322–5331. [CrossRef]
11. Nisar, M.; Sung, H.H.-Y.; Williams, I.D. Arylsulfonyl derivatives of 11-azaartemisinin: Approaching new polymorphs via seeds of molecular analogues. *Acta Crystallogr. Sect. A Found. Adv.* **2018**, *74*, a104. [CrossRef]
12. Parambil, J.V.; Poornachary, S.K.; Heng, J.Y.Y.; Tan, R.B.H. Template-induced nucleation for controlling crystal polymorphism: From molecular mechanisms to applications in pharmaceutical processing. *CrystEngComm* **2019**, *21*, 4122–4135. [CrossRef]
13. Nangia, A. Conformational Polymorphism in Organic Crystals. *Acc. Chem. Res.* **2008**, *41*, 595–604. [CrossRef]
14. Cruz-Cabeza, A.J.; Bernstein, J. Conformational Polymorphism. *Chem. Rev.* **2014**, *114*, 2170–2191. [CrossRef]
15. Haynes, R.K.; Wong, H.-N.; Lee, K.-W.; Lung, C.-M.; Shek, L.Y.; Williams, I.D.; Croft, S.L.; Vivas, L.; Rattray, L.; Stewart, L.; et al. Preparation ofN-Sulfonyl- andN-Carbonyl-11-Azaartemisinins with Greatly Enhanced Thermal Stabilities: In vitro Antimalarial Activities. *ChemMedChem* **2007**, *2*, 1464–1479. [CrossRef]
16. Trask, A.V.; Jones, W. Crystal Engineering of Organic Cocrystals by the Solid-State Grinding Approach. *Top. Curr. Chem.* **2005**, *254*, 41–70. [CrossRef]
17. Sheldrick, G.M. A short history of SHELX. *Acta Crystallogr. Sect. A Found. Crystallogr.* **2008**, *A64*, 112–122. [CrossRef]
18. Sheldrick, G.M. Crystal structure refinement with SHELXL. *Acta Crystallogr. Sect. C Struct. Chem.* **2015**, *C71*, 3–8. [CrossRef]

19. Dolomanov, O.V.; Bourhis, L.J.; Gildea, R.J.; Howard, J.A.K.; Puschmann, H. OLEX2: A complete structure solution, refinement and analysis program. *J. Appl. Cryst.* **2009**, *42*, 339–341. [CrossRef]
20. Bourhis, L.J.; Dolomanov, O.V.; Gildea, R.J.; Howard, J.A.K.; Puschmann, H. The anatomy of a comprehensive constrained, restrained refinement program for the modern computing environment-Olex2 dissected. *Acta Cryst. A Found. Crystallogr.* **2015**, *71*, 59–75. [CrossRef]
21. Parsons, S.; Flack, H.D.; Wagner, T. Use of intensity quotients and differences in absolute structure refinement. *Acta Crystallogr. Sect. B Struct. Sci. Cryst. Eng. Mater.* **2013**, *69*, 249–259. [CrossRef] [PubMed]
22. Douroumis, D.; Ross, S.A.; Nokhodchi, A. Advanced methodologies for cocrystal synthesis. *Adv. Drug Deliv. Rev.* **2017**, *117*, 178–195. [CrossRef] [PubMed]
23. Karki, S.; Friščić, T.; Fábián, L.; Jones, W. New solid forms of artemisinin obtained through cocrystallisation. *CrystEngComm* **2010**, *12*, 4038–4041. [CrossRef]
24. Watson, D.J.; Laing, L.; Gibhard, L.; Wong, H.N.; Haynes, R.K.; Wiesner, L. Toward New Transmission-Blocking Combination Therapies: Pharmacokinetics of 10-Amino-Artemisinins and 11-Aza-Artemisinin and Comparison with Dihydroartemisinin and Artemether. *Antimicrob. Agents Chemother.* **2021**, *65*, e00990-21. [CrossRef]
25. Kavanagh, O.N.; Croker, D.M.; Walker, G.M.; Zaworotko, M.J. Pharmaceutical cocrystals: From serendipity to design to application. *Drug Discov. Today* **2019**, *24*, 796–804. [CrossRef]
26. Schultheiss, N.; Newman, A. Pharmaceutical Cocrystals and Their Physicochemical Properties. *Cryst. Growth Des.* **2009**, *9*, 2950–2967. [CrossRef]
27. Etter, M.C.; Macdonald, J.C.; Bernstein, J. Graph-set analysis of hydrogen-bond patterns in organic crystals. *Acta Crystallogr. Sect. B Struct. Sci.* **1990**, *46*, 256–262. [CrossRef]
28. Cavallo, G.; Metrangolo, P.; Milani, R.; Pilati, T.; Priimagi, A.; Resnati, G.; Terraneo, G. The Halogen Bond. *Chem. Rev.* **2016**, *116*, 2478–2601. [CrossRef]
29. Spackman, P.R.; Turner, M.J.; McKinnon, J.J.; Wolff, S.K.; Grimwood, D.J.; Jayatilaka, D.; Spackman, M.A. CrystalExplorer: A program for Hirshfeld surface analysis, visualization and quantitative analysis of molecular crystals. *J. Appl. Crystallogr.* **2021**, *54*, 1006–1011. [CrossRef]
30. Taylor, C.R.; Day, G.M. Evaluating the Energetic Driving Force for Cocrystal Formation. *Cryst. Growth Des.* **2018**, *18*, 892–904. [CrossRef]
31. Steed, J.W. 21st century developments in the understanding and control of molecular solids. *Chem. Commun.* **2018**, *54*, 13175–13182. [CrossRef]
32. la Vega, A.S.-D.; Duarte, L.J.; Silva, A.F.; Skelton, J.M.; Rocha-Rinza, T.; Popelier, P.L.A. Towards an atomistic understanding of polymorphism in molecular solids. *Phys. Chem. Chem. Phys.* **2022**, *24*, 11278–11294. [CrossRef]
33. Thakore, S.D.; Sood, A.; Bansal, A.K. Emerging role of primary heterogeneous nucleation in pharmaceutical crystallization. *Drug Dev. Res.* **2020**, *81*, 3–22. [CrossRef]